Journal of Statistical Physics (2023) 190:16
https://doi.org/10.1007/s10955-022-03032-z

Thermalization of Isolated Harmonic Networks Under Conservative Noise

Stefano Lepri[1]

Received: 16 May 2022 / Accepted: 31 October 2022

Abstract
We study a scalar harmonic network with pair interactions and a binary collision rule, exchanging the momenta of a randomly-chosen couple of sites. We consider the case of the isolated network where the total energy is conserved. In the first part, we recast the dynamics as a stochastic map in normal modes (or action-angle) coordinates and provide a geometric interpretation of it. We formulate the problem for generic networks but, for completeness, also reconsider the translation-invariant lattices. In the second part, we examine the kinetic limit and its range of validity. A general form of the linear collision operator in terms of eigenstates of the network is given. This defines an *action network*, whose connectivity gives information on the out-of-equilibrium dynamics. We present a few examples (ordered and disordered chains and elastic networks) where the topology of connections in action spaces can be determined in a neat way. As an application, we consider the classic problem of relaxation to equipartition from the point of view of the dynamics of linear actions. We compare the results based on the spectrum of the collision operator with numerical simulation, performed with a novel scheme based on direct solution of the equations of motion in normal modes coordinates.

Keywords Equipartition · Harmonic network · Conservative noise · Master equation

1 Introduction

Nonequilibrium processes in many particle systems can be categorized in two wide classes: transport induced by external forces (either mechanical and thermodynamical) and relaxation to equilibrium. In the first class, we encounter steady-state transport, or even time-dependent states like it happens e.g. in surface growth, pattern formation, turbulent flows etc. The second class concerns problems like thermalization and approach to equipartition, coarsening,

Communicated by Keiji Saito.

✉ Stefano Lepri
stefano.lepri@isc.cnr.it

[1] Consiglio Nazionale delle Ricerche, Istituto dei Sistemi Complessi, via Madonna del piano 10, I-50019 Sesto Fiorentino, Italy

Published online: 12 November 2022

relaxation after a quench and so on. Both themes continue to receive a large attention and the goal is to categorize them in broad classes characterized by some form of universality.

The issue of thermalization has a long-standing history, starting with the classic Fermi–Pasta–Ulam–Tsingou problem [1] until the most recent developments, regarding the effect of integrability and quasi-integrability on the statistical behavior of classical systems [2–7].

One common trait in the study of such a problem is the difficulty of treating genuine anharmonic systems which are usually tackled by molecular dynamics simulations. This is the case of large ensembles of coupled nonlinear oscillators driven out of equilibrium [8–10]. Even in the weakly-nonlinear limit, perturbative methods like the KAM theory are notoriously of little use in thermodynamically-large systems. In the kinetic regime, approaches based on the phonon Boltzmann or wave-kinetic equation are well developed [11]. For one-dimensional chains this turned out to be useful to understand anomalous transport [12–15] and (pre)thermalization caused by nonlinear resonances [16, 17]

An alternative approach relies on stochastic modeling of the mesoscopic dynamics, where the toolbox of stochastic processes can be fruitfully used. Considerable insights is thereby obtained on the nature of the non-equilibrium states and macroscopic transport laws [18, 19].

An intermediate viewpoint is to consider a sort of hybrid dynamics, where a deterministic evolution is accompanied by stochastic interactions, possibly preserving the basic conservation laws. In the simplest case, the deterministic dynamics is linear and solvable, while the random part can be seen as is a microcanonical Monte-Carlo rule, ergodizing the dynamics. This is referred to as conservative noise dynamics: in its simplest versions it entails random exchange of momenta between particle or a random reshuffling of a subset of particles. Such schemes, allows sometimes for exact solutions or, at least, very efficient simulations. For fluid systems, this is the strategy of the Multi-Particle-Collision dynamics that can be fruitfully employed in many diverse contexts [20–22]. For the class of oscillator chains, this class of random dynamical systems allows for an exhaustive rigorous treatment [23–26]. Indeed, large-scale hydrodynamics equations can be demonstrated and phonon Boltzmann equation can be derived, yielding relatively simple linear collision operators [27, 28]. Moreover, most of nonequilibrium steady-state properties can be computed exactly [29–32] and were shown to reproduce many features of deterministic nonlinear lattices [33]. The effect of conservative noise on nonlinear oscillator chains has also been considered [24, 34–36].

Another ingredient is the effect of quenched disorder, leading to subtle interplay between Anderson localization and chaotic diffusion that affects both thermalization and transport [37–41]. A further motivation to tackle this case is that classical disordered chains with nonlinear interactions exhibit a regime analogous to that seen in quantum many-body-localized systems [42]. In addition to intrinsic heterogeneity of individual units, disorder can originate also from topology and structure of connections, as it occurs for the dynamics of elastic networks (see e.g. Ref. [43] and references therein). This type of structures have an intrinsic theoretical interest, and may serve, for instance, as toy models of macromolecules (e.g. proteins) in their native state [44, 45]. Another possible domain of application is the study of nanoscale heat transfer trough networked structures [46, 47], namely as toy models of devices composed of networks of nanowires and nanotubes.

When dealing with weakly-interacting linear systems it is natural to refer to the unperturbed harmonic modes and their energies or actions. For regular, homogeneous, anharmonic lattices these are the usual Fourier modes. Their perturbed dynamics determines the evolution of relevant observables both far [48] than close [49, 50] to equilibrium. For disordered lattices one has instead to consider Anderson modes that are typically localized in space.

Generally, when expressed in the familiar action-angle variables, a nonintegrable perturbation defines a network of interaction among the unperturbed actions [51, 52]. It is reasonable

to argue that the connectivity of such network will affect relaxation and ergodic properties. In general, one can distinguish such networks depending on whether the number of groups of actions linked by the perturbation depends intensively or extensively on the number of degrees of freedom N. These are termed short or long-range networks, respectively, depending on whether the coupling range if roughly constant or increases proportionally to N [51, 52]. In the nonlinear case the coupling may involve three or more actions, resulting in complicated hyper-graph structure. It is thus of interest to characterize the connectivity of such action network in the simplest setting, and this is one of the aims of the present paper.

In the present work, we present a general class of dynamical systems with conservative-noise: an harmonic network with general pair interaction described by a coupling matrix and equipped with a binary collision rule, exchanging the momenta of a couple of randomly chosen pair of particles. The motivations are twofold. First, we would like to understand how the conservative-noise dynamics translates in the space of collective coordinates (i.e. the eigenstates of the underlying harmonic network). In other words, how do local interactions in space affects the normal modes. Second, we would like to gain some insights on the connectivity and topology of the resulting action networks, in the simplest setting. We also focus on the problem of relaxation to equilibrium concentrating on the dynamics of linear actions, a subject that has not been considered so far for conservative noise dynamics.

In the first part, we recast the stochastic dynamics as a stochastic map in normal modes (or action-angle) coordinates and provide a geometric interpretation of it. We will formulate the problem on generic scalar networks but, for completeness, we will reconsider also the translation-invariant lattices. As a byproduct, we derive an efficient and novel scheme to integrate numerically the equations of motion in the collective coordinates.

In the second part, we examine the kinetic limit and its range of validity. We compute the linear collision operator in the normal mode basis and discuss a few examples where the topology of connections in action spaces can be discussed in a neat way. As an application, we study the classic problem of relaxation to equipartition *a lá* Fermi–Pasta–Ulam–Tsingou, starting from an initial condition with a few actions excited. We compare the exact dynamics with the kinetic results. A discussion and summary is given in the last section.

2 Harmonic Network with Conservative Noise

Let us consider the following quadratic Hamiltonian,

$$H = \sum_{i=1}^{N} \frac{p_i^2}{2m_i} + \frac{1}{2} \sum_{i,j=1}^{N} \Phi_{ij} q_i q_j, \tag{1}$$

where the matrix Φ is semi-positive definite and symmetric so that its eigenvalues are real and non-negative. The equation of motion of the isolated network are

$$\ddot{q}_i = -\sum_j \Phi_{ij} q_j \quad . \tag{2}$$

In order to have momentum conservation it must be $\sum_i \Phi_{ij} = 0$. For simplicity we will deal henceforth with the equal-mass case, and set $m_i = 1$.

We now introduce the following stochastic process [23]. Suppose we start with the system at time t. At a later time $t + \tau$ there occur a "collision" event defined as follows. A couple of particles $(m, n), m \neq n$ is randomly selected according to the joint probability $W_{n,m}$ and their momenta are exchanged, $(p_n, p_m) \to (p_m, p_n)$. Clearly, this move conserves energy and the

total momentum. Physically, it can be interpreted as a perfectly elastic collision as it would occur for a infinite square-well pair potential. In this general formulation, the model encompasses several different setups. It includes the standard case of regular Euclidean lattices when Φ is the familiar nearest-neighbor Laplacian matrix. The $W_{n,m}$ can be assigned to include some form of non-local interaction across the lattice. The intervals between subsequent collision times τ are also taken as random variables with some preassigned distribution with given, finite, average $\langle\tau\rangle$. A natural choice would be, for instance, the exponential distribution $\exp(-\tau/\langle\tau\rangle)/\langle\tau\rangle$.

The normal modes' coordinates of the network have eigenfrequencies ω_ν and are defined by the transformation

$$Q_\nu = \sum_{l=1}^{N} q_l \, \chi_l^\nu, \quad P_\nu = \sum_{l=1}^{N} p_l \, \chi_l^\nu. \tag{3}$$

The χ_l^ν, $\nu = 1, \ldots, N$, are orthornormal and can be taken to be real for the time being. Once the Hamiltonian is expressed in these new canonical variables, the deterministic part of the equations of motion become

$$\dot{Q}_\nu = \frac{\partial H}{\partial P_\nu} = P_\nu, \tag{4}$$

$$\dot{P}_\nu = -\frac{\partial H}{\partial Q_\nu} = -\omega_\nu^2 Q_\nu. \tag{5}$$

Let us now determine the dynamics associated to the random part. At each collision there is change in normal-mode momenta ΔP_ν given by

$$\Delta P_\nu = (p_m - p_n)(\chi_n^\nu - \chi_m^\nu)$$

while the Q are unchanged. Using the inverse of (3)

$$p_n = \sum_\nu P_\nu \chi_n^\nu, \quad p_m - p_n = \sum_\nu P_\nu (\chi_m^\nu - \chi_n^\nu)$$

we obtain

$$\Delta P_\nu = (\chi_n^\nu - \chi_m^\nu) \sum_\mu (\chi_m^\mu - \chi_n^\mu) P_\mu.$$

In the case in which Φ conserve the total momentum, momentum and stretch are automatically conserved since $\Delta P_0 = 0$. So one can work with a $N - 1$ variables. Altogether, in column vector notation, the collision rule can be written as

$$P' = P + \Delta P = (1 - 2VV^T)P, \tag{6}$$

$$V_\nu^{(n,m)} \equiv \frac{\chi_n^\nu - \chi_m^\nu}{\sqrt{2}}, \tag{7}$$

where the prime denotes the value after the collision and V^T the transpose. Note that $V = V^{(n,m)}$ is a random vector as the indexes n, m are chosen at random with the prescribed rule (unless needed, we do not write explicitly the dependence on the site indexes henceforth). It can be checked that the vector V is a unit vector, $V^T V = 1$. Thus, Eq. (7) has an interesting geometrical interpretation. Indeed, $(1 - 2VV^T)$ it is a Householder matrix that describes a reflection about an hyperplane containing the origin. The hyperplane is orthogonal to the vector V. So the dynamics can be seen as a sequence of reflections of the vector P around

a random hyper-plane in phase space, a transformation that conserves the vector length $|P|^2 = P^T P$. The matrix properties are well known:

- It is idempotent $(1 - 2VV^T)^2 = 1$;
- It is self adjoint $(1 - 2VV^T)^+ = (1 - 2VV^T)$;
- It has has one eigenvalue equal to -1 and the remaining $N - 1$ equal to 1.
- Also $\Delta P = -2VV^T P = -2(P^T V)V$ where $R = P^T V = |P| \cos\varphi$ is the projection of P on V so

$$P' = P - 2RV$$

Since $|\Delta P|/|P|$ is of order one, the change in each component is of order $1/\sqrt{N}$.

3 Equations for the Collective Variables

Let us now consider the dynamics in the usual action variables to understand how the above transformations affects their dynamics. Introducing

$$A = i(2\Omega)^{1/2} Q + (2\Omega)^{-1/2} P, \tag{8}$$

with $\Omega_{\nu\nu'} = \omega_\nu \delta_{\nu\nu'}$ (note that A_ν are $2N$ independent complex variables). The inverse formulae (recall that P, Q are assumed to be real):

$$P = \frac{1}{2}(2\Omega)^{1/2}\left(A + A^*\right); \quad Q = \frac{1}{2i}(2\Omega)^{-1/2}\left(A - A^*\right),$$

with Hamiltonian transforming to $H = A^+ \Omega A$. Substituting into (7) we obtain the collision map:

$$A' = A - M(A + A^*), \tag{9}$$

where the matrix M is defined as

$$M \equiv \Omega^{-1/2} V V^T \Omega^{1/2}; \qquad M_{\nu,\nu'} = \sqrt{\frac{\omega_{\nu'}}{\omega_\nu}}\, V_\nu V_{\nu'}$$

(V is real). The matrix M is real, not symmetric since from the definition $M^T = \Omega M \Omega^{-1}$ and is idempotent $M^2 = 1$ expressing the fact that applying twice the same transformation does not change the state.

For the collective variables, the free evolution in the time interval $(t, t + \tau)$ between subsequent collisions is diagonal

$$A(t + \tau) = e^{i\Omega\tau} A(t), \qquad A^*(t + \tau) = e^{-i\Omega\tau} A^*(t). \tag{10}$$

Combining the two processes (9) and (10), we obtain an exact map from t^+ to $(t + \tau)^+$

$$A \to (1 - M)e^{i\Omega\tau} A - M e^{-i\Omega\tau} A^*. \tag{11}$$

The evolution thus amounts to a sequence of multiplication of random matrices originating from the randomness of both the matrix M and of the collision intervals τ. This formulation is particularly useful for implementing the numerical solution as an event-driven dynamics, not requiring any approximate integration schemes as in the case of ordinary or stochastic differential equations (see Appendix A).

As a further step, we seek for the equations for the action-angle variables I, θ defined by $A_\nu = \sqrt{I_\nu} e^{i\theta_\nu}$. From Eq. (9) and recalling that M is real, we obtain the collision map

$$\begin{aligned} I'_\nu &= I_\nu - 4\sqrt{\frac{I_\nu}{\omega_\nu}} V_\nu Z \cos\theta_\nu + \frac{4V_\nu^2}{\omega_\nu} Z^2 \\ &= I_\nu \left[\sin^2\theta_\nu + \left(\cos\theta_\nu - \frac{2V_\nu}{\sqrt{\omega_\nu I_\nu}} Z \right)^2 \right] \\ \sin\theta'_\nu &= \sqrt{\frac{I_\nu}{I'_\nu}} \sin\theta_\nu \\ Z &\equiv \sum_\mu V_\mu \sqrt{\omega_\mu I_\mu} \cos\theta_\mu . \end{aligned} \tag{12}$$

- Those equations are exact: the first one guarantees that the energy is conserved at each collision as $\sum_\nu \omega_\nu \Delta I_\nu = 0$. Note however that the total action $\sum_\nu I_\nu$ *is not* a constant of motion.
- The transformation made the collision map nonlinear, and Z is global coupling among the eigenmodes: each collision entails a change of action and angles of all the modes.
- Finally, taking into account the free evolution, we can rewrite the dynamics as a mapping from t^- to $(t+\tau)^-$ (i.e. just before two subsequent collisions)

$$\begin{aligned} I &\to I + \Delta I(I, \theta) \\ \theta &\to \theta + \omega\tau + \Delta\theta(I, \theta), \end{aligned}$$

  where $\Delta I = I' - I$ and $\Delta\theta$ are defined by the (12) and ω is the vector of the eigenfrequencies ω_ν. It is a a kind of random mapping or discrete Langevin equation (but note that it is not symplectic).

Before proceeding further, we note that the calculation can be performed also rewriting the Eq. (9) as a suitable stochastic equation. The details are in Appendix B.

4 Kinetic Equation for the Actions

Let us now consider the kinetic limit, namely the case in which very many collisions occur on the time scale T, $T \gg \langle\tau\rangle$. The limit in which $N \to \infty$, $\langle\tau\rangle \to 0$ keeping

$$\gamma = \frac{1}{N\langle\tau\rangle} \tag{13}$$

finite, corresponds to choosing a finite collision probability per node of the network. This is the choice mostly employed in the simulations [31, 34, 36]. In this case, on the time-scale $T \sim 1/\gamma$ the number of collisions becomes macroscopically large. Qualitatively, the phases perform a random walk and are randomized on a faster time scale with respect to the evolution of the actions. We thus argue that the angles θ_ν are quickly randomized on this time scale and it is legitimate to average the first of (12) over a uniform distribution of θ, which is the expected invariant measure. Denoting by $\overline{I_\nu}$ such averaged actions we obtain

$$\overline{I'_\nu} = \left(1 - 2V_\nu^2\right) \overline{I_\nu} + 2\frac{V_\nu^2}{\omega_\nu} \sum_{\nu'} \omega_{\nu'} V_{\nu'}^2 \overline{I_{\nu'}}. \tag{14}$$

In other words, this last equation represents the evolution of an ensemble of trajectories with a given distribution of initial angles, subject to the *same sequence* of collisions. Equivalently, in terms of the mode energies, $E_\nu = \omega_\nu \overline{I}_\nu$:

$$E'_\nu = \left(1 - 2V_\nu^2\right) E_\nu + 2V_\nu^2 \sum_{\nu'} V_{\nu'}^2 E_{\nu'} \equiv E_\nu + \sum_{\nu'} K_{\nu,\nu'} E_{\nu'} \tag{15}$$

which, taking into account the normalization of V, shows immediately that the sum of the E_ν is conserved also for the averaged equations, and we have defined the angle-averaged collision matrix

$$K_{\nu,\nu'}^{(n,m)} = -2V_\nu^2 \delta_{\nu,\nu'} + 2V_\nu^2 V_{\nu'}^2. \tag{16}$$

Each of the matrices K has the following properties:

- It is a symmetric matrix and it is random as it depends on the couple of colliding particles (n, m). It does not seem to belong to any known ensemble of standard random matrices.
- It does not depend on the eigenfrequencies and the distribution of collision times but only on the eigemodes' shape and on the collision probabilities $W_{n,m}$.
- It is seen immediately that K admits a zero eigenvalue with uniform eigenvector $E_\nu = E_{eq}$ where E_{eq} is the energy value of each mode at equipartition.
- K is doubly-stochastic matrix, rows and columns sums to one.

We now would like to perform an average over realization of the collision process. The formal solution from t to $t + T$ is thus given in terms of a product of (uncorrelated) random matrices

$$E(t + T) = \left(\prod_{collisions(n,m)} \left(1 + K^{(n,m)}\right) \right) E(t) \tag{17}$$

(with 1 denoting here the identity matrix) and the product is extended to all the collision occurring in the time interval $[t, t + T]$. On the basis of the usual arguments based on Oseledec theorem, we thus expect that the associated Lyapunov exponents exist [53].

If each application of the collision rule yields a small change in the vector E (for instance if all elements of K are small), one can approximate the product in (17) as

$$\prod_{collisions(n,m)} \left(1 + K^{(n,m)}\right) \approx 1 + \sum_{collisions(n,m)} K^{(n,m)}. \tag{18}$$

This approximation is akin to the well-known weak-disorder expansion, a method used to evaluate the product of random matrices for small disorder strengths [53]. Its accuracy here will be afterwards checked numerically for the specific examples considered below. If we accept its validity for the time being we can, as a further step, replace the sum in (18) with the average $\overline{K}$ of the matrix over the random process. In other words, one considers the averaged operator coarse-grained over a time scale which is longer than the typical collision time:

$$\overline{K} = \sum_{(n,m)} W_{n,m} K^{(n,m)}, \quad R \equiv \frac{1}{\langle\tau\rangle} \overline{K} = \gamma N \overline{K}. \tag{19}$$

The rate γ just sets the overall time-scale of the kinetic process. The (constant) matrix $\overline{K}$ inherits the properties of the $K^{(n,m)}$. Altogether, replacing the differences in (17) with a time derivative, the relaxation processes on such time scale is given by

$$\dot{E}_\nu = \sum_{\nu'} \left[R_{\nu,\nu'} E_{\nu'} - R_{\nu',\nu} E_\nu \right]; \qquad R_{\nu,\nu'} \equiv \frac{2}{\langle\tau\rangle} \overline{V_\nu^2 V_{\nu'}^2}. \tag{20}$$

This equation thus provides the seeked effective approximate evolution of mode energies on a time scale where the network has undergone a large number of collisions. Since energy is conserved, Eq. (20) can be seen as a Master Equation in action space and the elements of R can be interpreted as transition rates from a state E to E'. They are of the form of the well-known Fermi golden rule, involving the squared amplitudes of the eigenmodes. For a generic coupling of the network, such that there is no decoupling among different subsets they are all nonvanishing. Following the usual arguments of Markov processes, the system is ergodic and approaches equipartition according to the properties of the "collision operator" defined by (20). So the thermalization problem reduces to computing its N eigenvalues μ_ν, $\nu = 1, \ldots, N$, whose absolute values give the spectrum of relaxation rates. The first eigenvalue $\mu_1 = 0$ and corresponds, as said, to the steady state of energy equipartition. On physical grounds, μ_1 must be non-degenerate since we expect the dynamics to be ergodic for a quadratic Hamiltonian with such collision rules. All the others μ_ν must be strictly negative [54]. In particular, it is of interest to look at the spectral gap $|\mu_2 - \mu_1| = |\mu_2|$ that controls the relaxation at long times in a finite network. The scaling with N of μ_2 (also called the Fiedler eigenvalue in the context of diffusion on graphs) can be recast in terms of the scaling of spectral density of the action network. Let us denote with $\rho(\mu)$ the integrated (cumulative) density of eigenvalues (i.e. the fraction of eigenvalues less than μ). If

$$\rho(\mu) \sim |\mu|^{d_\mu/2}, \qquad \mu \to 0 \tag{21}$$

one may estimate μ_2 for a finite network from the condition $\rho(\mu_2) = 1/N$, from which we obtain $|\mu_2| \sim N^{-d_\mu/2}$. Note that, on general grounds, d_μ is a distinct quantity from the standard spectral dimension d_s of the original network (1), which is defined by the same relation as (21) for the integrated density of eigenfrequencies ω_ν [55, 56].

Before proceeding further, let us comment on the validity of the weak-disorder approximations (18). It rests on the fact that the change of the energy vector is somehow small at each collision. This is plausibly true in the case of extended modes, as it occur in the case of translation-invariant or weakly disordered lattices that will be treated below: each χ is of order $1/\sqrt{N}$ for normalization. From the very definition of the V, Eq. (7), we see that the matrix elements of the relaxation matrix should be small for large N. In other words, each local collision (which yield a change $O(1)$ of the particle momenta) yield a $O(1/N)$ change of the mode energies. This expectation will be made precise in the standard case of the ordered chain (see Sect. 5).

On the other hand, this may not be true in general, e.g if the network admits localized modes. To understand this issue, let us consider the most trivial example in which Φ is diagonal with frequencies $\omega_\nu = \sqrt{\Phi}$ and trivial eigenvectors $\chi_m^\nu = \delta_{m,\nu}$ (assuming that they are labeled according to their spatial location). The matrix K can be worked out: it is all zeros except for two diagonal elements and two elements in positions (n, m), (m, n),

$$K_{\mu,\nu}^{(n,m)} = \begin{cases} -\frac{1}{2} & \text{if } (\mu, \nu) = (m, m), (n, n) \\ \frac{1}{2} & \text{if } (\mu, \nu) = (m, n), (n, m) \\ 0 & \text{otherwise.} \end{cases} \tag{22}$$

Thus, the matrix is very sparse with $O(1)$ entries, very different from the case of extended plane waves. However the change involves only one mode, thus resulting in a relatively small change of the vector E even in this case.[1]

[1] Actually, this extreme case is basically the well-known KMP model whereby harmonic oscillators exchange energy stochastically [18]. But, it may be also related to deterministic models like the linear chain of oscillators

For a general Φ the eigenvectors are not known analytically but can be easily computed numerically by exact diagonalization. Then, one can compute the matrix form of the collision operator by averaging over the chosen distribution $W_{n,m}$. The structure of the matrix will yield information on the structure of action network. An analytically treatable case is the one of ordinary lattices that we will discuss below.

5 Translation-Invariant Lattice

We now consider the case of a translation-invariant lattice, focusing on a one-dimensional chain with periodic boundary conditions. In this case of Φ is a circulant matrix: this is a well-studied case both for short (nearest-neighbour) [23] than for long-range interactions [59]. In both cases the eigenvectors are the familiar lattice Fourier modes

$$\chi_l^{\nu} = \frac{1}{\sqrt{N}} e^{ik_\nu l}; \quad V_\nu \equiv \frac{e^{ik_\nu n} - e^{ik_\nu m}}{\sqrt{2N}}$$

where $k_\nu = \frac{2\pi\nu}{N}$ are the wavenumbers and

$$Q_\nu = \frac{1}{\sqrt{N}} \sum_{l=1}^{N} q_l \, e^{ik_\nu l}, \qquad Q_{-\nu} = Q_\nu^*, \qquad \nu = -\frac{N}{2} + 1, \ldots, \frac{N}{2}. \tag{23}$$

(for simplicity of notation we use matrix indexes in the same range). A difference with the case above is that the vectors V are complex. This requires some minor modifications when expressing the equation of motion in phononic variables. As explained in Appendix A, the collision map (11) now reads

$$A \to (1 - M) e^{i\Omega\tau} A - M e^{-i\Omega\tau} \tilde{A}^*, \tag{24}$$

where we introduced the shorthand notation $(\tilde{A}^*)_\nu = A_{-\nu}$. This makes transparent how the collision involves scattering of phonons with opposite propagation directions. The matrix M is formally as before but is now complex-valued

$$M \equiv \Omega^{-1/2} V V^+ \Omega^{1/2}; \qquad M_{\nu,\nu'} = \sqrt{\frac{\omega_{\nu'}}{\omega_\nu}} \, V_\nu V_{\nu'}^* \tag{25}$$

and it is non-Hermitean and idempotent.

The collision map in action-angle variables is:

$$I'_\nu = I_\nu - 4\sqrt{\frac{I_\nu}{\omega_\nu}} Re\left(V_\nu e^{-i\theta_\nu}\right) Z + \frac{4|V_\nu|^2}{\omega_\nu} Z^2 = I_\nu \left| 1 - \frac{2V_\nu e^{-i\theta_\nu}}{\sqrt{I_\nu \omega_\nu}} Z \right|^2 \tag{26}$$

$$\sin\theta'_\nu = \sqrt{\frac{I_\nu}{I'_\nu}} \sin\theta_\nu - 2\frac{Im(V_\nu)}{\sqrt{\omega_\nu I'_\nu}} Z \tag{27}$$

$$Z \equiv \frac{1}{2} \sum_\mu \sqrt{\omega_\mu I_\mu} \left(V_\mu e^{-i\theta_\nu} + V_\mu^* e^{i\theta_\nu} \right)$$

(note that Z is real).

with hard-core collisions, termed the ding-dong model [57] in its disordered version [58]. It would correspond to the "stochastic approximation" of the dynamics whereby the deterministic sequence of collisions is replaced by a random one.

Accordingly, in the kinetic limit we can proceed with the averaging as above. The resulting kinetic equations are equal to (14, 15) and (16) with the V_ν^2 replaced by

$$|V_\nu|^2 = \frac{1}{2N}\left|1 - e^{ik_\nu(m-n)}\right|^2. \tag{28}$$

With respect to the general network, for linear chains there are some important simplifications.

1. In the standard case of nearest-neighbor collisions $m = n + 1$ so that the above quantity is independent of n, m

$$|V_\nu|^2 = \frac{1}{2N}\left|1 - e^{ik_\nu}\right|^2 = \frac{2}{N}\sin^2\frac{k_\nu}{2},$$

and the matrix K is constant. Note that this remains true even for any fixed-distance collision rule $l = m - n$. The collision operator is determined straightforwardly from definitions (13) and (19)

$$R_{\nu,\nu'} = \gamma N K_{\nu,\nu'} = -4\gamma \sin^2\frac{k_\nu}{2}\delta_{\nu,\nu'} + \frac{8\gamma}{N}\sin^2\frac{k_\nu}{2}\sin^2\frac{k_{\nu'}}{2} \tag{29}$$

Since the off-diagonal terms are small for large N, the eigenvalues of the matrix are well approximated by the diagonal elements giving the approximation

$$\mu_\nu \approx -4\gamma \sin^2\frac{\pi(\nu-1)}{N}, \tag{30}$$

up to higher-order corrections in $1/N$ that may be computed perturbatively. Also, the νth eigenvectors is localized on $\pm\nu$ with all other components being small of order $1/N$. Since the spectrum has a vanishing gap for large N, the relaxation rate of a generic non-equilibrium initial condition is expected to occur on of the slowest time scale $\mu_2 \approx \gamma(\pi/N)^2$ at long times.

2. A more general model would consist to consider a collision probability of the form

$$W_{n,m} = w_{n-m} \tag{31}$$

meaning that we choose an random particle n with equal probability and a neighbor at distance $l = n - m$ with probability w_l (with periodic boundary condition assumed), the standard case above being $w_l = \delta_{l,1}$. In this case, the matrix K is no longer constant. The averaged collision operator is expressed as

$$R_{\nu,\nu'} = \gamma N\overline{K}_{\nu,\nu'} = \gamma\sum_l w_l\left[-4\sin^2\frac{k_\nu l}{2} + \frac{8}{N}\sin^2\frac{k_\nu l}{2}\sin^2\frac{k_{\nu'} l}{2}\right] \tag{32}$$

which, as above, suggests the following approximation in terms of the diagonal elements

$$\mu_\nu \approx -4\gamma\sum_l w_l.\sin^2\frac{k_\nu l}{2}. \tag{33}$$

We will discuss an example later on.

Before concluding this section, we note that the choice of the w_l is crucial to assess the dependence of the μ_ν on the wavenumber k_ν, as seen already at the level of the approximation (33). In particular, introducing correlations and/or long-ranged rules may yield non-standard relaxation and transport depending on the range and correlation strengths. We will defer investigation of those issues to future works.

6 Examples

In this section we illustrate the above in some specific examples and check for the validity of the approximations done.

6.1 Disordered Chain

For a first test, let us consider the case of the harmonic chain with disorder in the pinning potential

$$H = \sum_{i=1}^{N} \left[\frac{{p_i}^2}{2} + \frac{1}{2}(1+\sigma_i) q_i^2 + \frac{1}{2}(q_{i+1} - q_i)^2 \right] \tag{34}$$

with σ_i being i.i.d. variables with uniform distributions in $[0, w]$, and w gauges the disorder strength. Periodic boundary conditions are assumed. As it is well known, the eigenstates are the exponentially-localized Anderson modes, whose localization length decreases with w [60, 61]. We consider the standard case of nearest-neighbor collisions. Several variants in this type of model have been considered earlier [62–64].

In Fig. 1 we illustrate the kinetic regimes for two cases corresponding to relatively weak and strong disorder. We first of all compute the relaxation spectrum as the Lyapunov exponents of the product or random matrices (17) via the usual QR algorithm [53]. Then, we compare the result with the eigenvalues of the averaged collision matrix as obtained from the weak-disorder expansion (18). In the case of weak disorder, Fig. 1a , the two methods give the same spectra, thus confirming the accuracy of the approximation. Moreover, the eigenvalues are also very close to the diagonal elements which, in turn, are almost indistinguishable from the one of the ordered case (see below). This means that the collision operator is almost diagonal with very small off-diagonal elements (see Fig. 1b).

The situation is different in the strong disorder case. Here, only first 25% of Lyapunov exponents coincide with the eigenvalues coincide and they are both very different from the diagonal elements (see Fig. 1c). This is presumably due to the fact that the dynamics is comparatively less "mixing" and stronger deviations from the average occur on shorter times (those corresponding to more negative Lyapunov exponents). Accordingly, the structure of the collision matrix is comparatively less homogeneous, with relatively larger off-diagonal elements (Fig. 1d).

A further insight is obtained by looking at the connectivity in action space. As said above, the transition rates are all-nonvanishing, but can be very small due to the exponential localization of the eigenvectors. For the sake of visualization, we draw a representation of action network as an adjacency matrix as follows. We consider two modes ν, ν' to be connected if $|R_{\nu,\nu'}|$ is larger than some preassigned threshold and not-connected otherwise. As seen in Fig. 2 there is a clear qualitative difference between the two cases: increasing disorder the connectivity decreases and passes from a complete-graph type to a more sparse structure. Accordingly, the degree distributions (the histogram of the number of links of each node) is distinctly different. For weak disorder, each action is connected to $O(N)$ ones, while the average degree is finite in the strong disorder case.

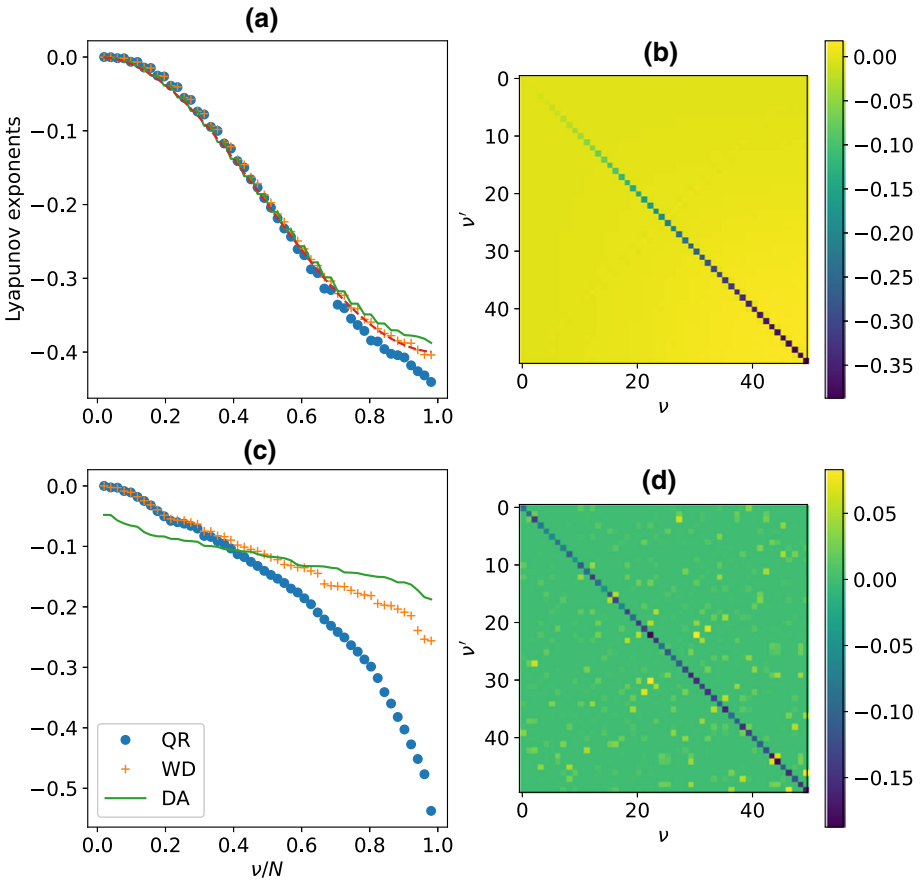

Fig. 1 Disordered chain (34), $N = 50$, $\gamma = 0.1$ with nearest neighbour collisions and disorder strengths $w = 0.1$ (**a**, **b**), $w = 10$ (**c**, **d**). **a**, **c** Report the Lyapunov exponents of Eq. (20): Circles are the numerical values computed via the QR algorithm, crosses are from the weak-disorder expansion [eigenvalues of the average matrix, as in Eq. (18)] The solid lines are the diagonal elements of the matrix itself. The dashed in (**a**) line are the diagonal elements in the case of no disorder $w = 0$ [Eq. (30)]. **b**, **d** Color plot of the averaged collision matrix (19) (Color figure online)

6.2 Mean-Field Chain

To test also the case of translation-invariant lattice we consider, for the sake of an example, a standard ordered chain with nearest-neighbour with an additional mean-field interaction:

$$H = \sum_{i=1}^{N} \left[\frac{{p_i}^2}{2} + \frac{1}{2}(q_{i+1} - q_i)^2 \right] + \frac{k}{2N} \sum_{ij} (q_i - q_j)^2. \tag{35}$$

This type of chains has been discussed as a model for Bose–Einstein condensate [65] and studied recently in a nonequilibrium setup [66, 67]. The eigenfrequencies are

$$\omega_\nu^2 \;=\; 2k + 4\sin^2\left(\frac{\pi\nu}{N}\right) \quad . \tag{36}$$

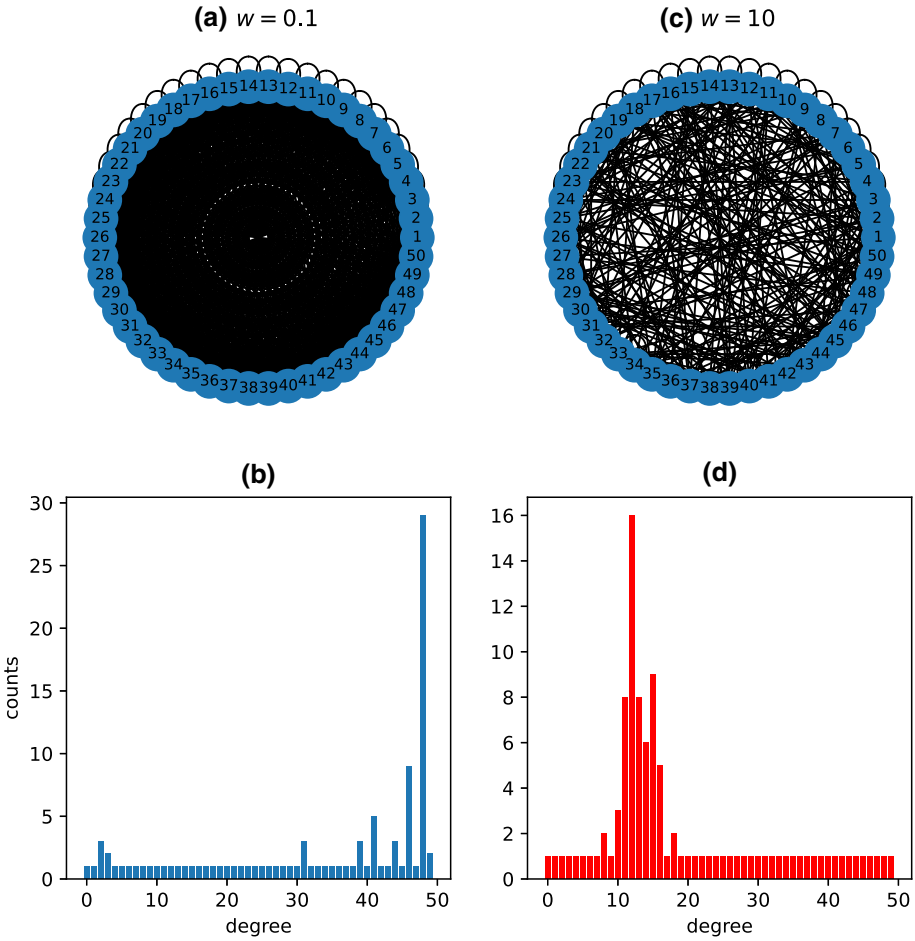

Fig. 2 Disordered chain (34), $N = 50$, $\gamma = 0.1$ with nearest neighbour collisions and disorder strengths $w = 0.1$ (**a**, **b**), $w = 10$ (**c**, **d**). **a**, **c** Graphical representation of the action network: it corresponds to an adjacency matrix where two nodes ν, ν' are consider to be connected if $|R_{\nu,\nu'}| > 10^{-4}$. **b**, **d** Degree distributions

for $\nu \neq 0$ and $\omega_0 = 0$. Apart from this zero mode, the dispersion is formally the same as the one of a chain with harmonic pinning.

As a result of the calculation in Sect. 5, the kinetic equations are independent on k (this will be checked later on). For the sake of testing the validity of the kinetic approximation, we here will concentrate on case $k = 0$, which is well-studied and sometimes referred to as the acoustic chain, since the dispersion of waves is linear for small wavenumbers. We will profit also to test the effect of different collision rules of type (31).

We first start with the relaxation rates obtained by the kinetic approximation. As above, we computed the spectrum numerically using the QR decomposition method [53] and compare it with the weak-disorder expansion and diagonal approximation. In Fig. 3 we report the relaxation rates computed with the different methods in two instances of (31) , namely the standard nearest-neighbor exchange and the one with a dichotomic choice between both the nearest and next-to-nearest neighbor, with probabilities s, $1 - s$ respectively,

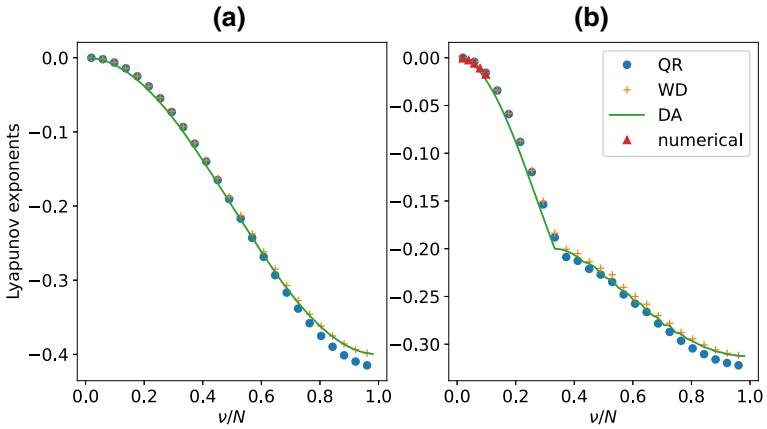

Fig. 3 Lyapunov exponents of Eq. (20) for the case of the translation-invariant acoustic chain (35) with $k = 0$, $N = 50$, $\gamma = 0.1$ and two types of for collision rule: among **a** nearest-neighbor and **b** nearest-neighbor and next-to-nearest neighbor sites with probability $s = 1/2$ each, Eq. (31. Circles are the numerical values of the Lyapunov exponents computed via the QR algorithm, crosses are from the weak-disorder expansion namely the eigenvalues μ_ν of the averaged matrix, as in Eq. (18). Solid lines are the diagonal approximation given by (30) and (33). To take into account the double degeneracy, only half of the exponents is plotted. Finally, the triangles are the relaxation rates measured from a simulation of a chain with the same parameters and $N = 128$ as described in Sect. 7

$$w_l = s\delta_{l,1} + (1-s)\delta_{l,2}. \tag{37}$$

In the first case, the matrix R is given by (29) while in the second we need to compute the Lyapunov spectra of the product of two constant matrices, randomly chosen with probability s. This correspond to the case of binary disorder in the random matrix language [53].

As illustrated in Fig. 3 the three methods agree fairly well for both collision rules. We examined also other values of k (data not reported) obtaining identical results as predicted. It should also be noticed that the diagonal approximation does reproduce quite accurately the spectrum already for $N = 50$.

6.3 Elastic Network

As an example of a more complicated topology, we consider a more general elastic network [43, 68]

$$H = \sum_{i=1}^{N} \left[\frac{{p_i}^2}{2} + \frac{1}{2}(q_{i+1} - q_i)^2 \right] + \frac{1}{2} \sum_{ij} C_{i,j}(q_i - q_j)^2, \tag{38}$$

where $C_{i,j} = 1$ if the nodes are connected and zero otherwise. As a case study, we choose the well-known Newman–Watts–Strogatz network, generated starting from a ring where each oscillator is coupled to its neighbor [69]. Each oscillator is then connected by to with randomly-chosen existing one with probability p. Increasing the probability p increases the level of disorder and we may expect a change the normal mode structure from extended plane-waves to localized. The spectral properties have been studied in great detail in [70]. The main feature is the existence of a pseudo-gap with very small eigenfrequencies below a certain value.

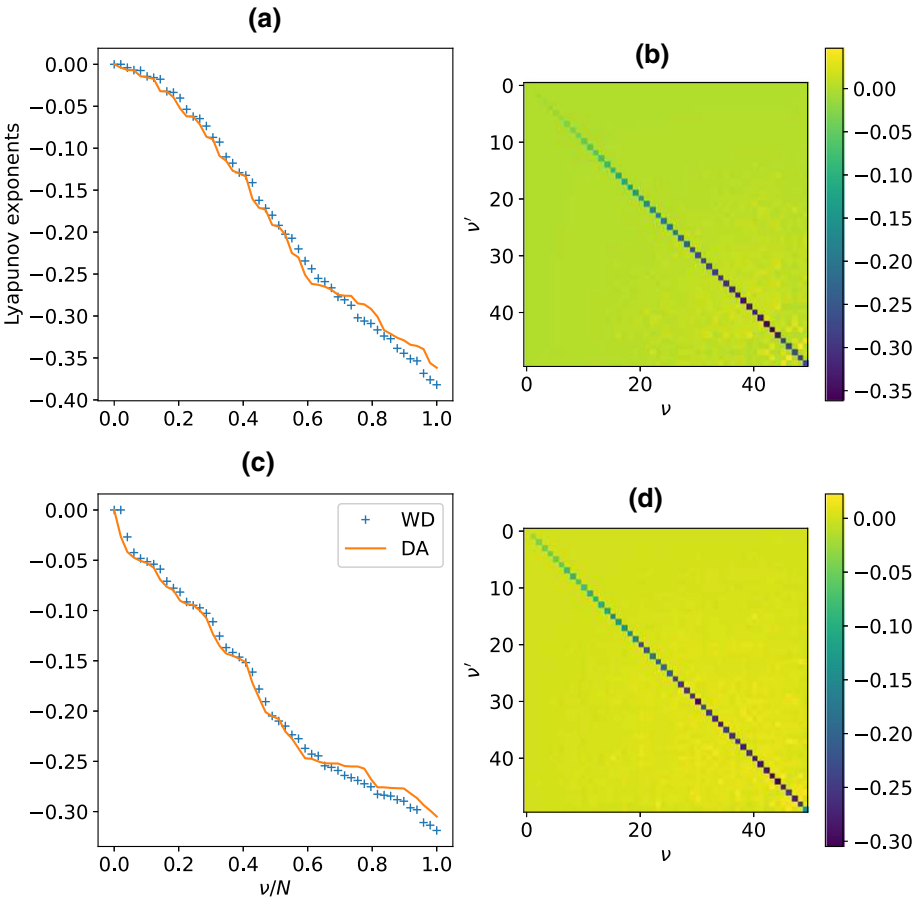

Fig. 4 Watts–Newman–Strogatz elastic network (38) $N = 50$, $\gamma = 0.1$ with nearest-neighbour collisions and $p = 0.1$ (**a**, **b**), $p = 0.8$ (**c**, **d**). **a**, **c** Report the Lyapunov exponents of Eq. (20): crosses are from the weak-disorder expansion (eigenvalues of the average matrix, as in Eq. (18)) The solid lines are the diagonal elements of the matrix itself. **b**, **d** Color plot of the averaged collision matrix (19) (Color figure online)

In Fig. 4 we compare for two cases corresponding to a single realization of $C_{i,j}$ and for relatively weak and strong disorder. We limit ourselves to compare the eigenvalues of the averaged collision matrix from the weak-disorder expansion (18) with the diagonal elements. In both examples, the two are pretty close, especially the smallest ones. This means that the collision operator is almost diagonal with very small off-diagonal elements, similar to the case of the strongly disordered chain.

In Fig. 5 we compare the degree distribution in the real network with the action network (as defined above) for two values of p. As it is well known, the degree distribution is peaked around the average value [69]. On the contrary, the action network, constructed as described above, is fully connected, with practically all-to-all couplings.

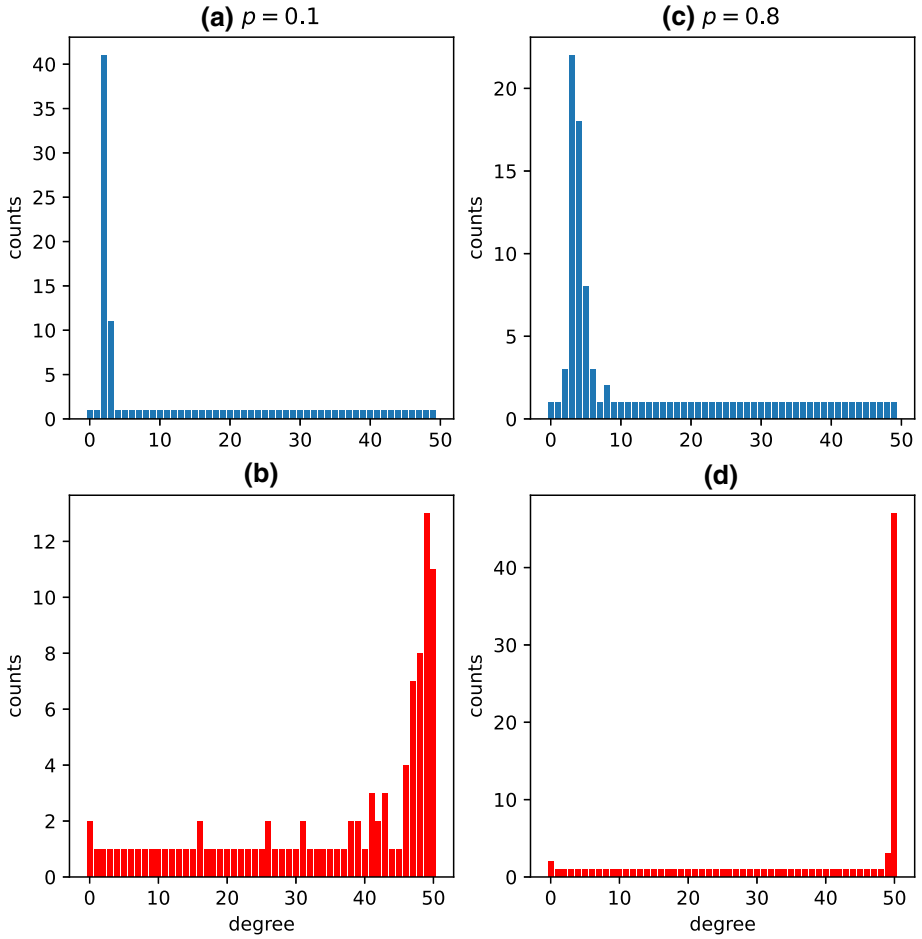

Fig. 5 Watts–Newman–Strogatz elastic network (34), $N = 50$, $\gamma = 0.1$ with nearest-neighbour collisions and $p = 0.1$ (**a**, **b**), $p = 0.8$ (**c**, **d**). Comparison of degree distributions in the real network (**a**, **b**) and in the the action network (**c**, **d**): it corresponds to an adjacency matrix where two nodes ν, ν' are considered to be connected if $|R_{\nu,\nu'}| > 10^{-4}$

7 Thermalization

We perform a thermalization simulation in the spirit of the Fermi–Pasta–Ulam–Tsingou famous numerical experiments. We initialize the chain by exciting a packet of N_0 normal modes to have a prescribed energy, namely we set

$$A_\nu(0) = \sqrt{\frac{E_0}{2N_0\omega_\nu}} e^{i\alpha_\nu} \tag{39}$$

for $0 < \nu \leq N_0$ ($|\nu| \leq N_0/2$, $\nu \neq 0$ in the case of translation-invariant chain) where α_ν being i.i.d.random phases uniformly distributed in $[0, 2\pi]$. The remaining modes are initialized as $A_\nu(0) = 0$. The dynamics is evolved iterating the dynamics as prescribed, with random Poissonian collision times whose average is given by (13).

The evolution of the mode energies E_ν towards equipartition is monitored and compared with the predictions. To improve the statistical accuracy a time-average over a fixed number of collision (typically 10^3) is performed, along with an average over different initial conditions, i.e. different realization of α_ν in (39). At long enough times, the average mode energies converge to the equipartition value as they should.

7.1 Disordered Chain

In Fig. 6 we report the simulation data of (34) for nearest-neighbor collisions and two values of the disorder parameter w, starting with all the energy fed into a few modes. In the upper panels we show the approach to equipartition of some of the excited modes. After an initial transient the decay sets to the exponential behavior with a rate that matches fairly well the value of the eigenvalue μ_2 (dashed lines). The mode evolution and repartition is illustrated in the lower panels. For weaker disorder, there is a steady transfer from the initial modes to the others that leads to a uniform depletion of their energies. On the other hand, for stronger disorder the transfer is in a sense, more irregular and involves modes with ν values different from ν_0. This is qualitative agreement with what we would expect in view of the different structures of the collision matrices as given in Figs. 1 and 2 and the different connectivity in action space.

Another observation from Fig. 6 is that the time scales involved are much smaller in the case of weaker disorder. To understand this issue, In Fig. 7a we compare the integrated spectral density $\rho(\mu)$ of (34) in the case with no disorder $w = 0$ and $w = 0.1$, and for different sizes. As expected, in the ordered case, $\rho \sim \sqrt{|\mu|}$, i.e $d_\mu = 1$. Remarkably, introducing a weak randomness ρ does approach zero for a finite μ., i.e the spectral gap is finite, meaning that $d_\mu = \infty$ and that the relaxation rate is finite and N-independent. This result should be however be taken with some care in the light of Fig. 7b that reports the integrated spectral density for stronger disorder. In the first case, the crossover to the $\sqrt{\mu}$ occurs at very small values of μ. It is thus possible that such a crossover will occur to smaller and smaller μ values upon decreasing the disorder, making d_μ converge to one in the thermodynamic limit.

To further characterize the effect of increasing disorder, in Fig. 8a we report the spectral gap for different lattice lengths as a function of w along with the average inverse participation ratio (Fig. 8b), defined as

$$IPR = \left[\frac{1}{N} \sum_{\nu} \sum_{n} \left| \chi_n^\nu \right|^4 \right]^{-1} \tag{40}$$

which is $O(1)$ for localized modes and $O(N)$ for extended ones. It thus gives a rough measure of the average localization length.

From the numerical data, it is seen that there exist a value $w_*(N)$ such that for $w < w_*$ the spectral gap is almost N-independent. This confirms that the relaxation is faster for weak enough disorder. On the other hand, for $w > w_*$ the spectral gap vanishes as N^{-2} (Fig. 8c). A possible argument to estimate the crossover value w_* is to identify it with the point at which the localization length becomes of the order the lattice size. Above such value some of the coefficients V_ν start to become exponentially small and the collision matrix more and more sparse accordingly. This estimate roughly correspond to the location of the maxima of $|\mu_2|$ in Fig. 8a. Indeed, using the average IPR as a measure of the localization length, we see that w_* should decrease with N, in qualitative agreement with the leftmost shifting of the maxima in Fig. 8a.

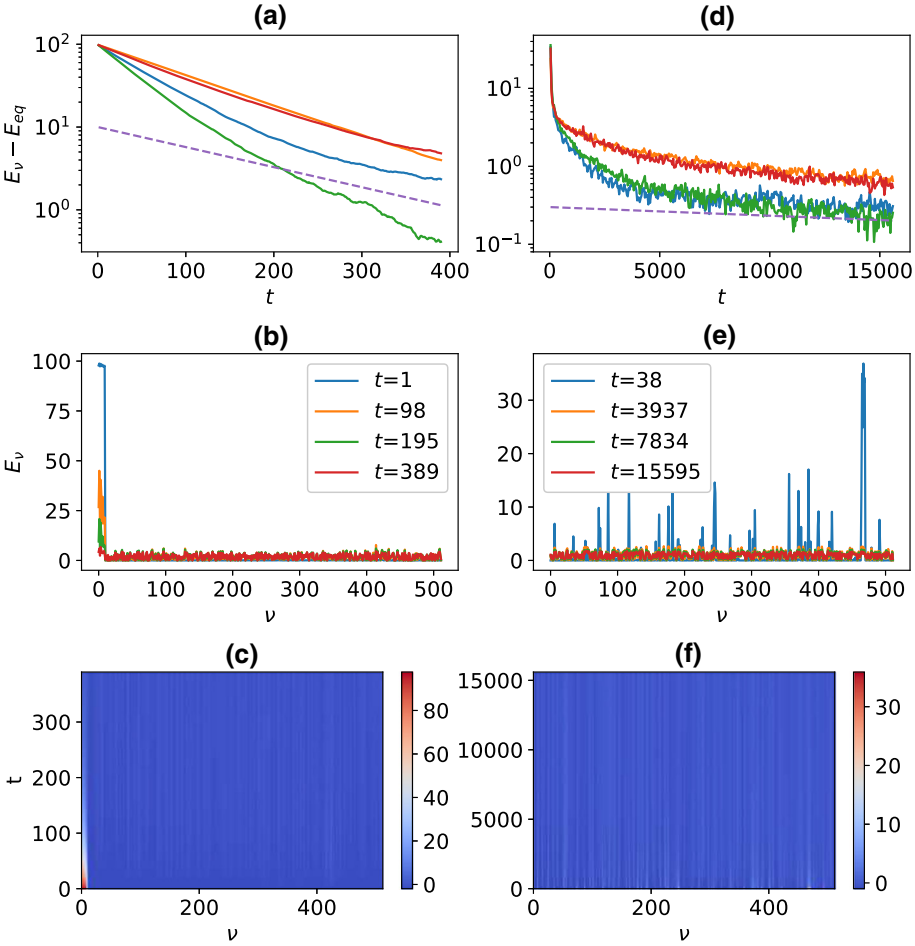

Fig. 6 Disordered chain (34), for $w = 2$ (left panels) $w = 10$ (right panels) $\gamma = 0.1$ with nearest-neighbor collisions. initial wavepacket lowest-frequency $N_0 = 5$ modes starting from $\nu = 0$ and 465 respectively. Upper panels (**a**, **d**): solid lines are $E_\nu(t) - E_{eq}$, dashed line corresponds to $0.3\exp(-|\mu_2|t)$. Middle (**b**, **e**): snapshots of the mode distributions at different times during the thermalization process. Lower panels (**c**, **f**): evolution of distributions $E_\nu(t)$ in mode space, equipartition corresponds to uniform color (up to fluctuations). Data are averaged over 2000 consecutive collisions and an ensemble of about 100 initial conditions, with different choices of α_ν in (39). Notice the difference in time scales between left and right panels

The $1/N^2$ scaling of the spectral gap suggests that the thermalization is ruled by some form of diffusive process in action space. This can be understood qualitatively as follows. In the strong disorder case, $w \to \infty$, one can to a first approximation, neglect the coupling in (34) and consider the eigenmodes as localized on a single site. We are thus in close to the case of independent oscillators and the matrix K can be approximated, up to exponentially small terms, by (22). So, considering the case of nearest-neighbor collisions, we argue that, up to a re-ordering of the eigenmodes indexes ν by their spatial positions, (20) is approximated as

$$\dot{E}_\nu = \frac{\gamma}{2}(E_{\nu+1} + E_{\nu-1} - 2E_\nu), \tag{41}$$

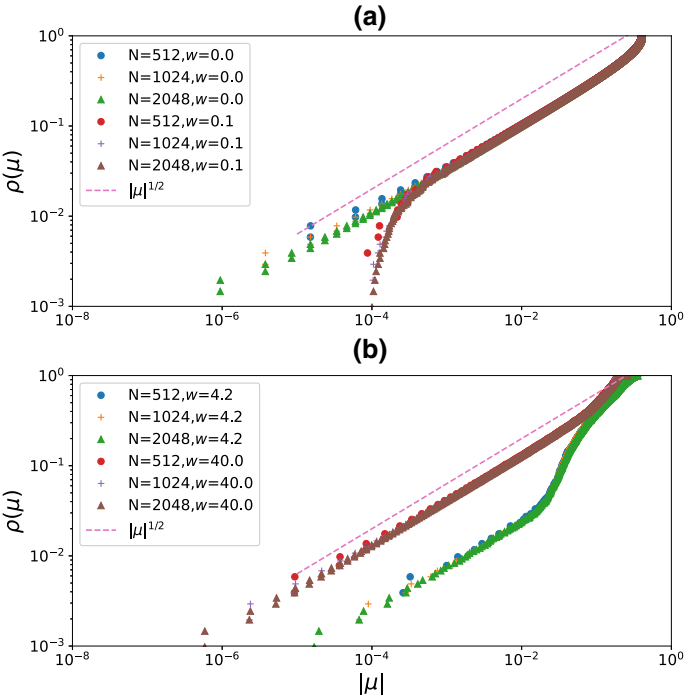

Fig. 7 The integrated spectral densities $\rho(\mu)$ (i.e. the fraction of eigenvalues less than μ) of the collision operator for model (34). Plots are for different disorder strengths and three lattice sizes $N = 512, 1024, 2048$; $\gamma = 0.1$ case with nearest-neighbor collisions. **a** Weak disorder: Comparison between with $w = 0$ (ordered case) and $w = 0.1$, and sizes $N = 512, 1024, 2048$; **b** Intermediate and strong disorder, $w = 4.2, 40$. The dashed line correspond to the scaling $\sqrt{|\mu|}$ expected for the ordered lattice

which immediately shows that the relaxation is a Brownian diffusion process in action space. Thus thermalization starting from a bunch of nearby modes would entail an initial growth of the number of excited modes proportional to $\sqrt{\gamma t}$. For a finite chain the longest time scale is given by the smallest eigenvalue of (41) which is of order $\gamma(2\pi/N)^2/2$. This is consistent with the scaling of μ_2 as given in Fig. 8.

Before passing to the next example, we mention the work [71] where a kinetic theory in a weakly-disordered nonlinear Schrödinger chain in the regime of homogeneous chaos. The regime there considered, is the one of weak enough interaction for the normal modes of the linear problem to remain well resolved but strong enough for the dynamics to be chaotic for almost all modes. In that case, the kinetic equations are nonlinear, leading to nonlinear diffusion [71].

7.2 Mean-Field Chain

Let us now consider again model (35). In Fig. 9 we report the data for the case for the acoustic chain with $k = 0$ and nearest-neighbor collisions. The relaxation of the four lowest modes is plotted in Fig. 9a, b along with the snapshots of the evolution of mode energy distributions in wavenumber space (Fig. 9c, d). The simulation data are in excellent agreement with the relaxation rates computed within the kinetic approach.

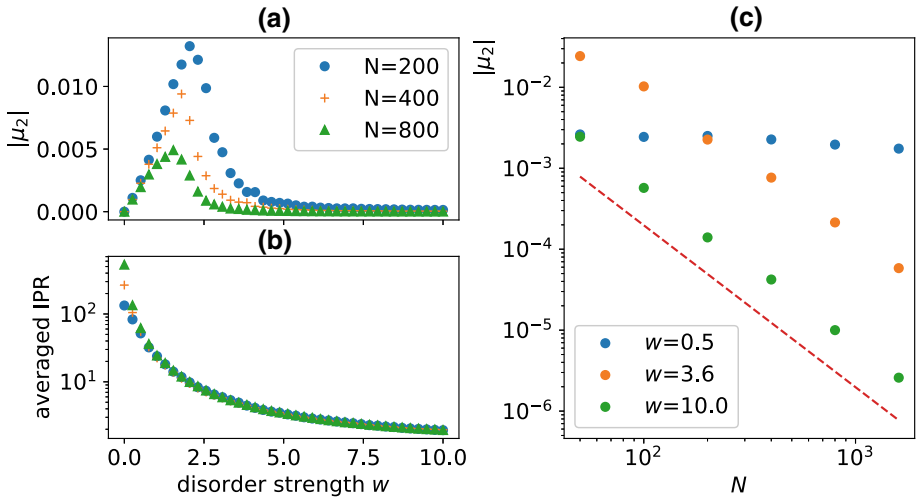

Fig. 8 Disordered chain (34), $\gamma = 0.1$ with nearest-neighbor collisions. **a** The absolute value of the second eigenvalue μ_2 of the averaged collision matrix (19) and **b** the average inverse participation ratio (40) as a function of disorder strength for different chain lengths; **c** reports the dependence of the eigenvalue on the lattice size N for different w. The dashed line correspond to the smallest non-zero eigenvalue of (41), $\gamma(2\pi/N)^2/2$

From the plots it is seen that thermalization occurs by gradual transfer of the energy from the excited modes towards all the others. Indeed, the energy in the whole background increases steadily and equipartition is reached with an overall rate $\mu_2 \sim 1/N^2$ as predicted.

We also tested the case with collision probability given by (37) obtaining similar results. In Fig. 3 we plot as red triangles the relaxation rates obtained by exponential fitting of $E_v(t)$: the agreement is again very good.

As said, the kinetic equation in this translation-invariant should be independent of k, if the the collision probability $W_{n,m}$ is the same. Thus, we simulated the model for different k maintaining the collisions only among nearest neighbors In Fig. 9b we confirm this expectation comparing the relaxation of the first Fourier mode for three different cases.

7.3 Elastic Network

For the Newman–Watts–Strogatz network (38) we limit ourselves to examine the spectral gap of the collision operator for different disorder strengths and different number of sites. We just give a first account, leaving a more complete study of such class of networks to future work.

For each N we consider a fixed random realization of the coupling matrix $C_{i,j}$ and change the probability p. A few different realizations of the couplings were examined with qualitatively similar results indicating that sample-to-sample fluctuations may not be very relevant. In Fig. 10a we compare the integrated spectral density $\rho(\mu)$ of (34) for different sizes and p. The data are compatible with a finite spectral gap for $p > 0$, and accordingly $d_\mu = \infty$, yielding a finite and N-independent relaxation rate.

In Fig. 11a, b we plot the spectral gap as a function of p along with the IPR. The situation is similar to the disordered chain in the weak-disorder regime see again Fig. 8. The spectral

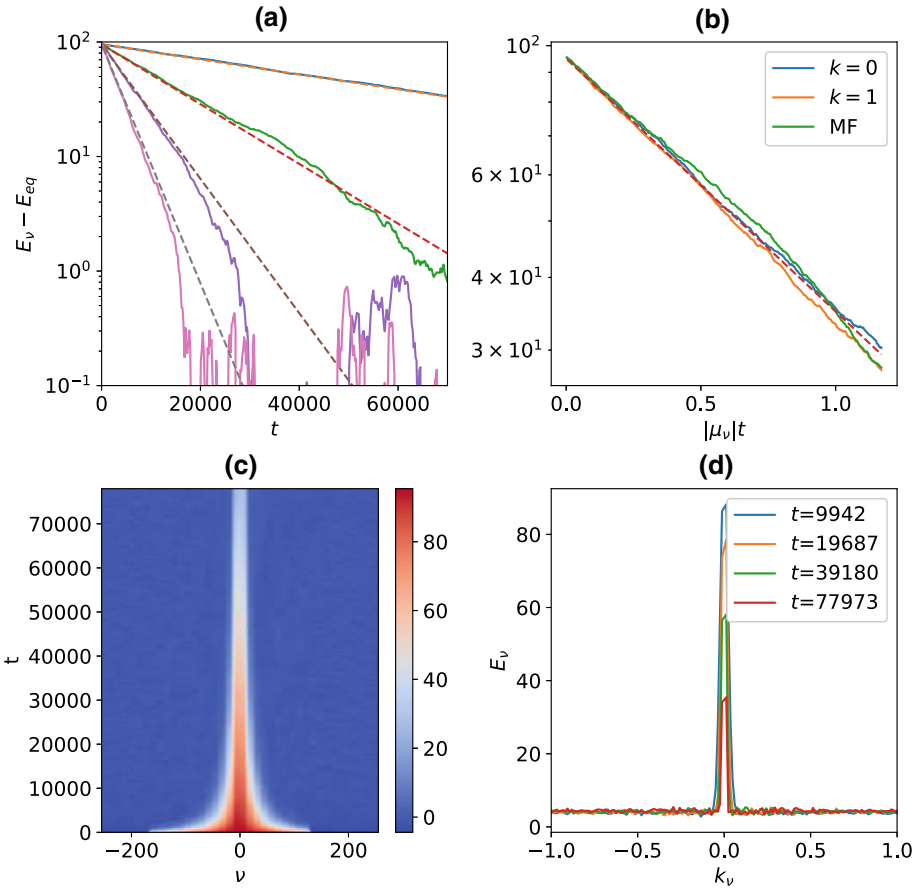

Fig. 9 Simulations of relaxation to equipartition for the chain (35) with nearest-neighbor collisions, $k = 0$, $N = 512$, $\gamma = 0.1$: initial wavepacket consisting of lowest-frequency $N_0 = 20$ modes. **a** Evolution of $E_\nu - E_{eq}$ the four lowest modes Dashed lines are exponential $95\exp(-|\mu_\nu|t)$ with rates μ_ν given by the approximation (30); plot of dynamics in mode space (**c**) and snapshots (**d**) of the mode distribution during the thermalization. **b** Evolution of the first mode $E_1 - E_{eq}$ as a function of $\mu_\nu t$ for $k = 0$, $k = 1$ and pure mean-field coupling, dashed line is $95\exp(-|\mu_2|t)$. Data are averaged over 10,000 consecutive collisions and over an ensemble of about 100 initial conditions, with different choices of α_ν in (39)

gap is finite for any finite p and closes for $p \to 0$. We do not observe a crossover to $1/N^2$ or similar scaling as in the case of the disordered chain.

8 Spectral Entropy

A key indicator that has been often employed to characterize the thermalization is the non-equilibrium (Shannon) spectral entropy [72]

$$S(t) = -\sum_\nu E_\nu \log E_\nu; \qquad \sum_\nu E_\nu = 1, \tag{42}$$

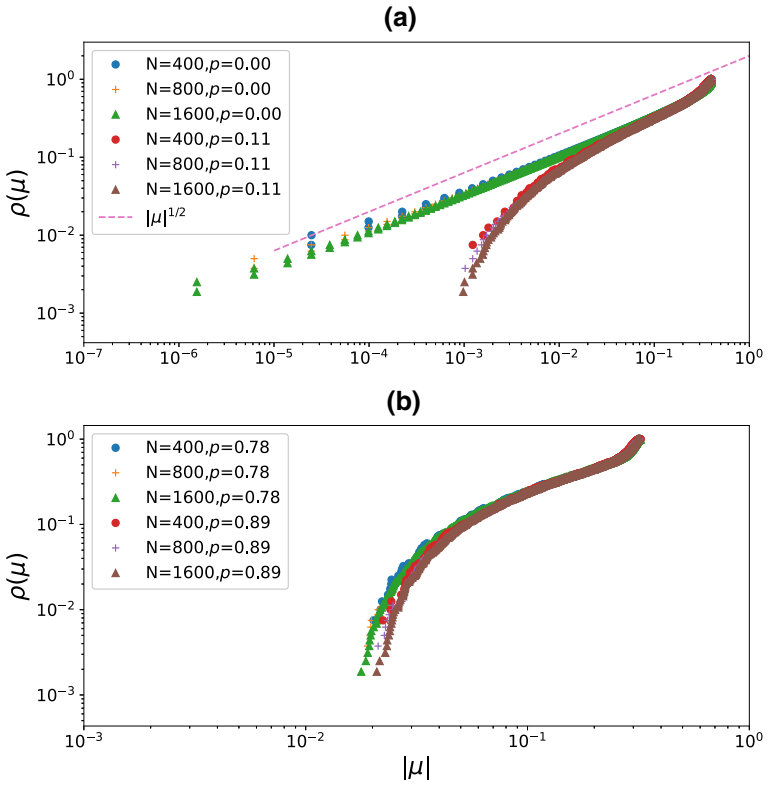

Fig. 10 The integrated spectral densities $\rho(\mu)$ of the collision operator (i.e. the fraction of eigenvalues less than μ) for the Newman–Watts–Strogatz lattices for different p and three lattice sizes $N = 512, 1024, 2048$; $\gamma = 0.1$ case with nearest-neighbor collisions. **a** Comparison between $p = 0$ (ordered case) and $p = 0.11$, and sizes $N = 400, 800, 1600$; The dashed line correspond to the scaling $\sqrt{|\mu|}$ expected for the ordered lattice. **b** Intermediate and strong disorder, $p = 0.78, 0.89$

where we have fixed the total energy to one, without loosing generality. For large t, S approaches its equipartition value $\log N$. In general S will depend on the initial conditions.

As we have shown above, the energy transfer processes in the translation-invariant models occurs through a gradual, global, redistribution of the initial energy towards all the other modes. In the intermediate times, and assuming all the energy initially in one single mode $E_{\nu_0}(0) = \delta_{\nu,\nu_0}$ for simplicity, one could thus perform a kind of "mean-field" approximation [73]. By this we mean that the energy of the initially excited mode is evenly redistributed among the other $N - 1$ ones, namely $E_\nu \approx (1 - E_{\nu_0})/(N - 1)$ for $\nu \neq \nu_0$ yielding the approximation

$$S(t) \approx S_{MF} \equiv -E_{\nu_0} \log E_{\nu_0} - (1 - E_{\nu_0}) \log \left(\frac{1 - E_{\nu_0}}{N - 1} \right) \tag{43}$$

where $E_{\nu_0}(t) \approx (1-1/N) \exp(-\mu_{\nu_0} t)+1/N$. In Fig. 12 we plot the simulated time evolution of S for the harmonic and disordered chains. The above formula accounts very well for the data.

The situation is instead pretty different in the case of the strongly disordered chain (see the full circles in Fig. 12b). Here, the action network is different yielding a diffusive process. Thus

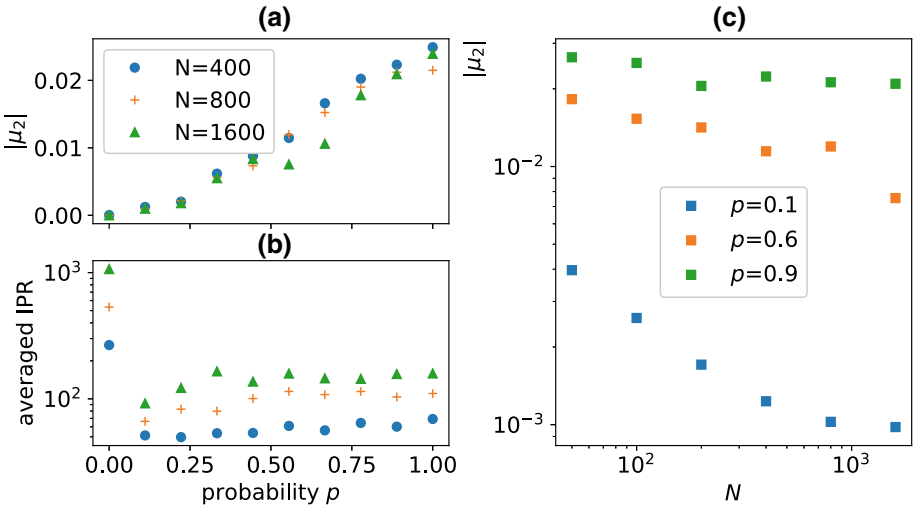

Fig. 11 Newman–Watts–Strogatz network (38), $\gamma = 0.1$ with nearest-neighbor collisions. **a** The absolute value of the second eigenvalue μ_2 of the averaged collision matrix (19) and **b** the average inverse participation ratio (40) as a function of disorder strength for different chain lengths; **c** reports the dependence of the eigenvalue on the lattice size N for different w

the entropy grows logarithmically in the intermediate time range. This is readily understood since, as said above, the number of excited modes grows as a $\sqrt{t}$. This fits with the general fact, that there exist a close relation between the growth of S and the spectrum of the master equation for diffusion on networks. In this context, it is known that if the spectral density of the Laplacian operator of the graph shows scaling with a finite spectral dimension d_s, the Shannon entropy grows as $\frac{d_s}{2} \log t$ with time before reaching the steady-state (uniform) value (see e.g. [73] and the references therein) .

9 Discussion and Perspectives

The conservative-noise dynamics for binary collision is a succession of random reflections in action space, see Eqs. (7) and (9). Averaging over random phases yield a kinetic equations for the actions/energies of normal modes. The mathematical advantage of such dynamics is that the collision operator is linear and yields a linear master equation (20). But the main merit, for our purposes, is that it was possible to construct explicitly the action network in term of the eigenvectors and the collision rule.

Being a stochastic model there is no doubt that equipartition will be finally obtained and that ergodicity is insured. However, one has the possibility to study relaxation of an arbitrary finite network by simply computing the spectral gap and its dependence on N. This amounts primarily to understand how the spectral density of the action network depends on the underlying connections. We also note that momentum conservation does not appear to play a major role for thermalization. For instance, both the case of strongly disordered case and the translation-invariant lattices display the same $1/N^2$ scaling of relaxation rates, despite the fact that momentum is conserved only in the second case.

Some comments are in order to conclude.

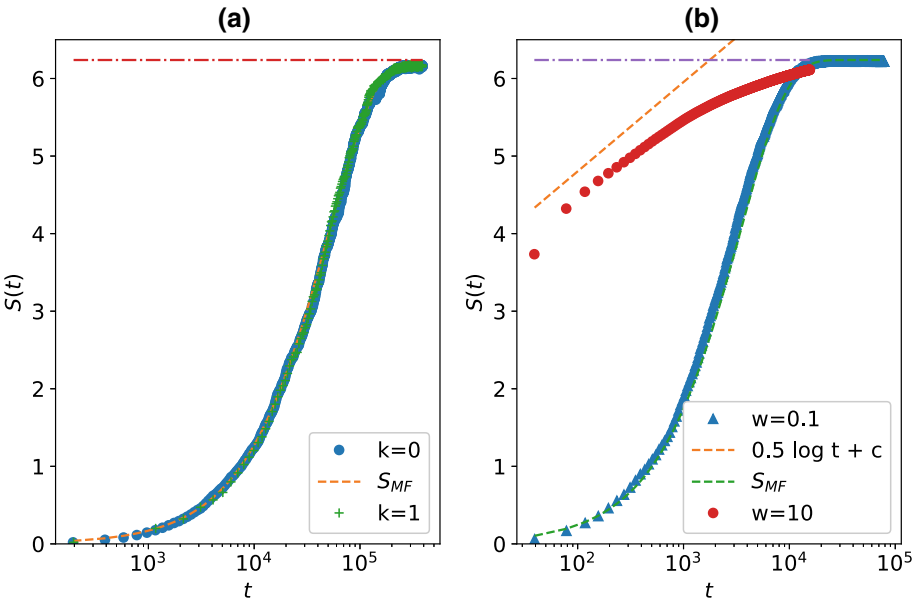

Fig. 12 Spectral entropy (42), $\gamma = 0.1$, $N = 512$ for the harmonic and disordered chains with nearest-neighbor collisions. **a** Model (35) with $k = 0, 1$ and **b** (34) with two values of the disorder. Initial conditions with only the lowest frequency mode is excited. Dashed lines correspond to the approximation (43); dot-dashed (red and violet) horizontal lines correspond to the equipartition value $S = \log N$ (Color figure online)

- The spectral density $\rho(\mu)$ of the collision operator for small μ is the main ingredient determining the the equipartition time in a finite network, see (21). A natural question is whether there exist a relation between d_μ and the spectral dimension in the case in which Φ of the harmonic network in (35) is Laplacian matrix. In general, we surmise that the two may not be necessarily related. This is understood in the case of the translation-invariant chain. There, d_μ is controlled by the collision rule only, as seen from (33) and can, in principle, be changed independently of the spectral dimension the Laplacian. However, we have seen that for the disordered chain that the relation is less straightforward and this issue may deserve a further analysis.
- To what extent are the present results applicable to describe a genuine nonlinear network? One may guess that the stochastic dynamics it is an idealization of a regime where chaos is well developed (i.e. the maximal Lyapunov exponent is very large) and homogeneous in space. This would occur for very large energy densities and/or strongly nonlinear networks. If so, correlations should decay rapidly and replacing local chaos by random collisions would be a reasonable assumption. It is also plausible that the overall structure of the action network may be described in the same language as here, although with higher-order connectivities (i.e. on a hyper-graph). This is a problem that deserves further studies.
- In the translation-invariant case the kinetic equation is basically the spatially-homogeneous version of the well-known phonon Boltzmann equation (or Boltzmann–Peierls equation) or wave-kinetic equation for phonon distribution [11, 16]. The main difference is that the random dynamics does not conserve the total number (i.e $\sum_\nu I_\nu$ in our notation). As it is known, a more general derivation yields an advection term, proportional to the phonon group velocity [11]. For the harmonic chain with conserving noise, it has been derived

in [27] with a more rigorous approach based on the Wigner distribution. The difference in our case is that we consider the mode energies and, more importantly, we dealt from the very start with the homogeneous case, whereby the energy distribution is initially spatially uniform and it remains so a later times. The inclusion of such terms is crucial to derive the correct hydrodynamic scaling, leading to correct (fractional) heat equation [74] on longer time-scales (see [25] and references therein for details).

- Also, in the language of phonon kinetic theory, a nonlinear potential of order x^p induces interaction involving p phonons. To the extent in which the random collisions here described represent an hard-core potential, namely an "infinite-order" $p \to \infty$ potential, it is thus understandable why the phonon modes are globally coupled. An important difference is also that, in the standard framework, energy and momentum conservation imposes constraints on the allowed phonon processes: (for example conditions like $\omega_w = \omega_k \pm \omega_q$ for three-phonons collisions etc.).
- In this work we focused on relaxation to equipartition of the isolated network. As it is well-known there is a close relation between relaxation close to equilibrium and transport. The relaxation rates can be used to predict the correlation decay, and thus the transport coefficients. The existence of a finite spectral gap of the collision operator is an indication of fast correlation decay which, in turn, imply normal diffusive transport. In the model we discussed this is relatively straightforward once the relaxation matrix is known. It remains to be investigated how its spectral properties depend on the underlying connections of the action network.
- One may wonder if the same approach can be applied to other systems with more conserved quantities. A relevant example would be the tight-binding electron problem, modeled as a discrete Schroedinger equation. In this case the collision rule should preserve both energy and the total wavefunction norm. However, it has been shown that this requires a nonlinear rule [75]. Thus the mathematical advantages following from the linearity are lost.

The class of models considered here will allow to extend the study of non-equilibrium properties to the case of open networks interacting with external reservoirs [76]. We plan to continue this program in the future.

Acknowledgements I thank Raffaella Burioni, Stefano Iubini, Francesco Piazza and Antonio Politi for useful correspondences and discussions during elaboration of this work.

Funding This work did not receive any funding.

Data Availability The datasets generated during and/or analysed during the current study are available from the corresponding author on reasonable request.

Appendix A: Translation-Invariant Model

Using (8) we can proceed with the calculation as before except for the fact that the normal coordinates Q, P are complex:

$$A_\nu = i(2\omega_\nu)^{1/2} Q_\nu + (2\omega_\nu)^{-1/2} P_\nu \tag{44}$$

$$A^*_{-\nu} = -i(2\omega_\nu)^{1/2} Q_\nu + (2\omega_\nu)^{-1/2} P_\nu, \tag{45}$$

and the inverse formulae now read:

$$P = \frac{1}{2}(2\Omega)^{1/2}\left(A + \tilde{A}^*\right),$$

where we introduced the shorthand notation $(\tilde{A})_\nu = A_{-\nu}$. Substituting into (7):

$$A' = A - \Omega^{-1/2} V V^+ \Omega^{1/2}\left(A + \tilde{A}^*\right) \equiv (1 - M)A - M\tilde{A}^*, \tag{46}$$

where the matrix M is given by (25). Using Eq. (10) for the free evolution and noticing that $\tilde{A}^* = e^{-i\Omega\tau}\tilde{A}^*(t)$ we obtain (24).

As stated in the text, the formulation of the equation of motion in the normal modes coordinates is very convenient for the implementation of the numerical solution. Taking into account the form of the matrix M and that $V^*_\nu = V_{-\nu}$ one can write the collision map as

$$A' = A - U(W^+ A + W^T A^*) \tag{47}$$

where the auxiliary vectors (of size N) are

$$U_\nu = V_\nu \sqrt{\frac{2}{\omega_\nu}}, \qquad W_\nu = V_\nu \sqrt{2\omega_\nu}$$

which is convenient for memory allocation as it requires only products of one-dimensional arrays at each collision. Free evolution (10) can be equally implemented as a product if one-dimensional arrays since Ω is diagonal. Therefore this scheme ensures exact energy and momentum conservation.

Appendix B: Stochastic Equations

It is useful to rewrite (11) as a stochastic equation. Writing $M \to M dw$ where $dw(t)$ is a stochastic process, which take the value 0 or 1 at random times, with the Poisson process satisfying $\langle dw \rangle = dt/\langle\tau\rangle$. The infinitesimal changes in the variables from time t to $t + dt$ to leading order is

$$dA = i\Omega A dt - M\left(A + A^*\right) dw, \tag{48}$$

where $dw^2 = dw$ has been used. For the translation-invariant case instead

$$dA = i\Omega A dt - M\left(A + \tilde{A}^*\right) dw, \tag{49}$$

(see the main text), with the same meaning of dw.

Equation (48) can be used to determine the equation for the action vector $I = A \circ A^*$, where $\circ$ is the Hadamard product (element-wise $A_\nu A^*_\nu = I_\nu$) with stochastic calculus. Dropping $dt^2, dtdw$ terms and using again $dw^2 = dw$:

$$d(A \circ A^*) = dA \circ A^* + dA^* \circ A + \frac{1}{2} dA \circ dA^* \tag{50}$$

$$= [-M\left(A + A^*\right) \circ \left(A + A^*\right) + M\left(A + A^*\right) \circ M\left(A + A^*\right)]dw,$$

which contains quadratic, non-diagonal terms. For completeness, we mention that stochastic equations have been discussed before for conservative noise, for instance for weakly interacting anharmonic oscillators [77]. Here, however, we deal with stochastic dynamics in action space.

In the kinetic limit, we proceed as in the main text. We first perform averaging over uniform random phases so that only diagonal terms survive $A_\nu A_\nu^* = I_\nu$ in the right-hand side. We get the stochastic equation for the actions

$$dI = 2\left[M \circ M - \mathrm{diag}(M)\right] I\, dw, \tag{51}$$

with $\mathrm{diag}(M)$ being the diagonal matrix with diagonal elements $M_{\nu,\nu}$ (again the same symbol I is used for the averages). Alternatively, we can work with the the mode energies defined, in matrix notation, as $E = \Omega I$:

$$dE = K E\, dw. \tag{52}$$

Equations (14) and (15) are of course equivalent to the above stochastic differential equation formulation.

References

1. Gallavotti, G.: The Fermi–Pasta–Ulam Problem: A Status Report, vol. 728. Springer, Berlin (2007)
2. Benettin, G., Christodoulidi, H., Ponno, A.: The Fermi–Pasta–Ulam problem and its underlying integrable dynamics. J. Stat. Phys. **152**(2), 195–212 (2013)
3. De Roeck, W., Huveneers, F.: Asymptotic localization of energy in nondisordered oscillator chains. Commun. Pure Appl. Math. **68**(9), 1532–1568 (2015)
4. Huveneers, F.: Classical and quantum systems: transport due to rare events. Ann. Phys. **529**(7), 1600384 (2017)
5. Fu, W., Zhang, Y., Zhao, H.: Nonintegrability and thermalization of one-dimensional diatomic lattices. Phys. Rev. E **100**(5), 052102 (2019)
6. Goldfriend, T., Kurchan, J.: Equilibration of quasi-integrable systems. Phys. Rev. E **99**(2), 022146 (2019)
7. Baldovin, M., Vulpiani, A., Gradenigo, G.: Statistical mechanics of an integrable system. J. Stat. Phys. **183**(3), 1–16 (2021)
8. Dhar, A.: Heat transport in low-dimensional systems. Adv. Phys. **57**, 457–537 (2008)
9. Lepri, S. (ed.): Thermal Transport in Low Dimensions: From Statistical Physics to Nanoscale Heat Transfer, Volume 921 of Lecture Notes in Physics. Springer-Verlag, Berlin Heidelberg (2016)
10. Benenti, G., Lepri, S., Livi, R.: Anomalous heat transport in classical many-body systems: overview and perspectives. Front. Phys. **8**, 292 (2020)
11. Spohn, H.: The phonon Boltzmann equation, properties and link to weakly anharmonic lattice dynamics. J. Stat. Phys. **124**(2), 1041–1104 (2006)
12. Pereverzev, A.: Fermi–Pasta–Ulam β lattice: Peierls equation and anomalous heat conductivity. Phys. Rev. E **68**(5), 056124 (2003)
13. Nickel, B.: The solution to the 4-phonon Boltzmann equation for a 1D chain in a thermal gradient. J. Phys. A **40**(6), 1219–1238 (2007)
14. Lukkarinen, J., Spohn, H.: Anomalous energy transport in the FPU-β chain. Commun. Pure Appl. Math. **61**(12), 1753–1786 (2008)
15. Lukkarinen, J.: Kinetic theory of phonons in weakly anharmonic particle chains. In: Thermal Transport in Low Dimensions, pp. 159–214. Springer, Cham (2016)
16. Onorato, M., Vozella, L., Proment, D., Lvov, Y.V.: Route to thermalization in the α-Fermi–Pasta–Ulam system. Proc. Natl. Acad. Sci. USA **112**(14), 4208–4213 (2015)
17. Huveneers, F., Lukkarinen, J.: Prethermalization in a classical phonon field: slow relaxation of the number of phonons. Phys. Rev. Res. **2**(2), 022034 (2020)
18. Kipnis, C., Marchioro, C., Presutti, E.: Heat flow in an exactly solvable model. J. Stat. Phys. **27**, 65 (1982)

19. Derrida, B.: An exactly soluble non-equilibrium system: the asymmetric simple exclusion process. Phys. Rep. **301**(1), 65–83 (1998)
20. Malevanets, A., Kapral, R.: Mesoscopic model for solvent dynamics. J. Chem. Phys. **110**, 8605–8613 (1999)
21. Kapral, R.: Multiparticle collision dynamics: simulation of complex systems on mesoscales. Adv. Chem. Phys. **40**, 89–146 (2008)
22. Di Cintio, P., Livi, R., Lepri, S., Ciraolo, G.: Multiparticle collision simulations of two-dimensional one-component plasmas: anomalous transport and dimensional crossovers. Phys. Rev. E **95**, 043203 (2017)
23. Basile, G., Bernardin, C., Olla, S.: Momentum conserving model with anomalous thermal conductivity in low dimensional systems. Phys. Rev. Lett. **96**, 204303 (2006)
24. Basile, G., Delfini, L., Lepri, S., Livi, R., Olla, S., Politi, A.: Anomalous transport and relaxation in classical one-dimensional models. Eur. Phys. J. Spec. Top. **151**, 85–93 (2007)
25. Basile, G., Bernardin, C., Jara, M., Komorowski, T., Olla, S.: Thermal conductivity in harmonic lattices with random collisions. In: Thermal Transport in Low Dimensions, pp. 215–237. Springer, Cham (2016)
26. Bernardin, C., Kannan, V., Lebowitz, J.L., Lukkarinen, J.: Harmonic systems with bulk noises. J. Stat. Phys. **146**(4), 800–831 (2012)
27. Basile, G., Olla, S., Spohn, H.: Energy transport in stochastically perturbed lattice dynamics. Arch. Ration. Mech. Anal. **195**(1), 171–203 (2010)
28. Lukkarinen, J., Marcozzi, M., Nota, A.: Harmonic chain with velocity flips: thermalization and kinetic theory. J. Stat. Phys. **165**(5), 809–844 (2016)
29. Lepri, S., Mejia-Monasterio, C., Politi, A.: Stochastic model of anomalous heat transport. J. Phys. A **42**, 025001 (2009)
30. Lepri, S., Mejia-Monasterio, C., Politi, A.: Dynamics of anomalous heat transport. J. Phys. A **43**, 065002 (2010)
31. Delfini, L., Lepri, S., Livi, R., Mejia-Monasterio, C., Politi, A.: Nonequilibrium dynamics of a stochastic model of anomalous heat transport: numerical analysis. J. Phys. A **43**(14), 145001 (2010)
32. Kundu, A., Bernardin, C., Saito, K., Kundu, A., Dhar, A.: Fractional equation description of an open anomalous heat conduction set-up. J. Stat. Mech.: Theory Exp. **2019**(1), 013205 (2019)
33. Lepri, S., Politi, A.: Density profiles in open superdiffusive systems. Phys. Rev. E **83**(3), 030107 (2011)
34. Iacobucci, A., Legoll, F., Olla, S., Stoltz, G.: Thermal conductivity of the Toda lattice with conservative noise. J. Stat. Phys. **140**(2), 336–348 (2010)
35. Bernardin, C., Goncalves, P.: Anomalous fluctuations for a perturbed Hamiltonian system with exponential interactions. Commun. Math. Phys. **325**(1), 291–332 (2014)
36. Lepri, S., Livi, R., Politi, A.: Too close to integrable: crossover from normal to anomalous heat diffusion. Phys. Rev. Lett. **125**(4), 040604 (2020)
37. Pikovsky, A.S., Shepelyansky, D.L.: Destruction of Anderson localization by a weak nonlinearity. Phys. Rev. Lett. **100**(9), 094101 (2008)
38. Kopidakis, G., Komineas, S., Flach, S., Aubry, S.: Absence of wave packet diffusion in disordered nonlinear systems. Phys. Rev. Lett. **100**(8), 084103 (2008)
39. Skokos, Ch., Krimer, D.O., Komineas, S., Flach, S.: Delocalization of wave packets in disordered nonlinear chains. Phys. Rev. E **79**(5), 056211 (2009)
40. Lepri, S., Schilling, R., Aubry, S.: Asymptotic energy profile of a wave packet in disordered chains. Phys. Rev. E **82**(5), 056602 (2010)
41. Basko, D.M.: Weak chaos in the disordered nonlinear Schroedinger chain: destruction of Anderson localization by Arnold diffusion. Ann. Phys. **326**(7), 1577–1655 (2011)
42. Kumar, M., Kundu, A., Kulkarni, M., Huse, D.A., Dhar, A.: Transport, correlations, and chaos in a classical disordered anharmonic chain. Phys. Rev. E **102**(2), 022130 (2020)
43. Bouchaud, J.-P., Georges, A.: Anomalous diffusion in disordered media: statistical mechanisms, models and physical applications. Phys. Rep. **195**(4–5), 127–293 (1990)
44. Tirion, M.M.: Large amplitude elastic motions in proteins from a single-parameter, atomic analysis. Phys. Rev. Lett. **77**(9), 1905 (1996)
45. Juanico, B., Sanejouand, Y.-H., Piazza, F., De Los Rios, P.: Discrete breathers in nonlinear network models of proteins. Phys. Rev. Lett. **99**(23), 238104 (2007)
46. Freitas, N., Paz, J.P.: Analytic solution for heat flow through a general harmonic network. Phys. Rev. E **90**(4), 042128 (2014)
47. Xiong, K., Zeng, C., Liu, Z., Li, B.: Influence of the degree of a complex network on heat conduction. Phys. Rev. E **98**(2), 022115 (2018)
48. Benettin, G., Ponno, A.: Time-scales to equipartition in the Fermi–Pasta–Ulam problem: finite-size effects and thermodynamic limit. J. Stat. Phys. **144**(4), 793 (2011)

49. Lepri, S.: Relaxation of classical many-body Hamiltonians in one dimension. Phys. Rev. E **58**(6), 7165–7171 (1998)
50. Lepri, S.: Memory effects and heat transport in one-dimensional insulators. Eur. Phys. J. B **18**(3), 441–446 (2000)
51. Mithun, T., Kati, Y., Danieli, C., Flach, S.: Weakly nonergodic dynamics in the Gross–Pitaevskii lattice. Phys. Rev. Lett. **120**(18), 184101 (2018)
52. Danieli, C., Mithun, T., Kati, Y., Campbell, D.K., Flach, S.: Dynamical glass in weakly nonintegrable Klein–Gordon chains. Phys. Rev. E **100**, 032217 (2019)
53. Pikovsky, A., Politi, A.: Lyapunov Exponents: A Tool to Explore Complex Dynamics. Cambridge University Press, Cambridge (2016)
54. Schnakenberg, J.: Network theory of microscopic and macroscopic behavior of master equation systems. Rev. Mod. Phys. **48**(4), 571 (1976)
55. Burioni, R., Cassi, D.: Universal properties of spectral dimension. Phys. Rev. Lett. **76**(7), 1091 (1996)
56. Burioni, R., Cassi, D.: Random walks on graphs: ideas, techniques and results. J. Phys. A **38**(8), R45 (2005)
57. Prosen, T., Robnik, M.: Energy-transport and detailed verification of Fourier heat law in a chain of colliding harmonic-oscillators. J. Phys. A **25**(12), 3449–3472 (1992)
58. Pikovsky, A.: Scaling of energy spreading in a disordered ding-dong lattice. J. Stat. Mech.: Theory Exp. **2020**(5), 053301 (2020)
59. Tamaki, S., Saito, K.: Energy current correlation in solvable long-range interacting systems. Phys. Rev. E **101**(4), 042118 (2020)
60. Matsuda, H., Ishii, K.: Localization of normal modes and energy transport in the disordered harmonic chain. Prog. Theor. Phys. Suppl. **45**, 76 (1970)
61. Visscher, W.M.: Localization of normal modes and energy transport in disordered harmonic chain. Prog. Theor. Phys. **46**(3), 729 (1971)
62. Bernardin, C.: Thermal conductivity for a noisy disordered harmonic chain. J. Stat. Phys. **133**(3), 417–433 (2008)
63. Dhar, A., Venkateshan, K., Lebowitz, J.L.: Heat conduction in disordered harmonic lattices with energy-conserving noise. Phys. Rev. E **83**(2), 021108 (2011)
64. Bernardin, C., Huveneers, F., Olla, S.: Hydrodynamic limit for a disordered harmonic chain. Commun. Math. Phys. **365**(1), 215–237 (2019)
65. Yan, J.: Harmonic interaction model and its applications in Bose–Einstein condensation. J. Stat. Phys. **113**(3), 623–634 (2003)
66. Defaveri, L., Olivares, C., Anteneodo, C.: Heat flux in chains of nonlocally coupled harmonic oscillators: mean-field limit. Phys. Rev. E **105**, 054149 (2022)
67. Andreucci, F., Lepri, S., Ruffo, S., Trombettoni, A.: Classical and quantum harmonic mean-field models coupled intensively and extensively with external baths. SciPost Phys. Core **5**(3), 036 (2022)
68. Hastings, M.B.: Random vibrational networks and the renormalization group. Phys. Rev. Lett. **90**(14), 148702 (2003)
69. Newman, M.E.J., Watts, D.J.: Renormalization group analysis of the small-world network model. Phys. Lett. A **263**(4–6), 341–346 (1999)
70. Monasson, R.: Diffusion, localization and dispersion relations on small-world lattices. Eur. Phys. J. B **12**(4), 555–567 (1999)
71. Basko, D.M.: Kinetic theory of nonlinear diffusion in a weakly disordered nonlinear Schroedinger chain in the regime of homogeneous chaos. Phys. Rev. E **89**(2), 022921 (2014)
72. Livi, R., Pettini, M., Ruffo, S., Sparpaglione, M., Vulpiani, A.: Equipartition threshold in nonlinear large Hamiltonian systems: the Fermi–Pasta–Ulam model. Phys. Rev. A **31**(2), 1039 (1985)
73. Mülken, O., Heinzelmann, S., Dolgushev, M.: Information dimension of stochastic processes on networks: relating entropy production to spectral properties. J. Stat. Phys. **167**(5), 1233–1243 (2017)
74. Dhar, A., Kundu, A., Kundu, A.: Anomalous heat transport in one dimensional systems: a description using non-local fractional-type diffusion equation. Front. Phys. **7**, 159 (2019)
75. Iubini, S.: Coupled transport in a linear-stochastic Schroedinger equation. J. Stat. Mech.: Theory Exp. **2019**(9), 094016 (2019)
76. Cuneo, N., Eckmann, J.-P., Hairer, M., Rey-Bellet, L.: Non-equilibrium steady states for networks of oscillators. Electron. J. Probab. **23**, 1–28 (2018)
77. Liverani, C., Olla, S.: Toward the Fourier law for a weakly interacting anharmonic crystal. J. Am. Math. Soc. **25**(2), 555–583 (2012)